Available online at www.sciencedirect.com

ScienceDirect

Journal of Magnesium and Alloys 10 (2022) 2510–2515

www.elsevier.com/locate/jma

Full length article

Unexpected high-temperature brittleness of a Mg-Gd-Y-Ag alloy

Lirong Xiao[a], Xuefei Chen[a,b], Huiyan Ning[c], Ping Jiang[b], Yi Liu[a], Bin Chen[d], Dongdi Yin[e,*], Hao Zhou[a,*], Yuntian Zhu[a,f]

[a] *Nano and Heterogeneous Materials Center, School of Materials Science and Engineering, Nanjing University of Science and Technology, Nanjing 210094, China*

[b] *State Key Laboratory of Nonlinear Mechanics, Institute of Mechanics, Chinese Academy of Sciences, Beijing 100190, China*

[c] *School of Mechanical and Electrical Engineering, Heilongjiang Institute of Technology, Harbin 150050, China*

[d] *ThermoFisher Scientific, Shanghai 201210, China*

[e] *Key Laboratory of Advanced Technologies of Materials, Ministry of Education, School of Materials Science and Engineering, Southwest Jiaotong University, Chengdu, Sichuan 610031, China*

[f] *Department of Materials Science and Engineering, City University of Hong Kong, Hong Kong 999077, China*

Received 3 March 2021; received in revised form 15 May 2021; accepted 14 June 2021

Available online 29 July 2021

Abstract

Rare earth (RE) can produce excellent precipitation hardening in Mg alloys. However, when forming a solid solution, it also deteriorates formability, a problem that can usually be overcome by raising deformation temperature. Here we report an unexpected observation of high temperature brittleness in a Mg-Gd-Y-Ag alloy. As the temperature reached 500 °C, the formability decreased drastically, leading to severe intergranular fracture under only 0.5% strain. This was caused by failure of grain boundaries, which are weakened by segregated interfacial compounds.

Keyword: Interfacial compounds; Formability; High temperature brittleness; Grain boundary sliding.

1. Introduction

Environmental pollution and energy source exhaustion are becoming severe crises that threat the well-being of humanity. As the lightest metallic materials, magnesium and its alloys have potential applications in many industries such as automobile, ship-building and aerospace [1–3]. Extensive investigations on alloy design, forming technology and deformation mechanism of wrought Mg alloys have been carried out to expand their applications in load-bearing components [4–9]. Especially, it has been found that the Mg-RE alloys can be effectively strengthened by age hardening [10–12], in which the dispersed nano precipitates block the slip of dislocations to enhance strength [13–16]. In addition, it has been reported that other strengthening mechanisms, such as grain refinement and solid solution, can also improve the strength of Mg-RE alloys in conjunction with precipitation hardening [17,18].

Industrial applications of Mg alloys are severely hindered by their poor formability at room temperature [19,20]. In addition, dislocation pinning by solution atoms in Mg-RE alloys further deteriorates their formability [21,22]. Therefore, high temperature deformations, which can activate more slip systems, are frequently employed to process Mg-RE alloys [23–25], although RE addition has negative effects on grain refinement in Mg alloys, which leads to higher critical temperatures for recrystallization [26,27] and changes of deformation mechanisms [28,29]. Recrystallization is known as effective way to reduce the dislocation density and consequently improve formability during hot deformation.

* Corresponding authors.
E-mail addresses: ahnydd@swjtu.edu.cn (D. Yin), hzhou511@njust.edu.cn (H. Zhou).

https://doi.org/10.1016/j.jma.2021.06.018

In this work, the deformation behaviors of Mg-Gd-Y-Ag alloy at a series of elevated temperatures were comparatively studied. It is found that the critical recrystallization temperature of Mg-Gd-Y-Ag alloy is ~440 °C. Stable rolling deformation to 80% of thickness reduction without any cracking was successfully achieved at this temperature. However, to our surprise, we found unexpected brittleness when the alloy was deformed at higher temperature of 500 °C. Severe cracking occurred in the sample that was rolled for only 0.5% of thickness reduction. This interesting phenomenon is against our current understanding of hot deformation. It is widely accepted that increasing temperature promotes the plastic deformation of most Mg alloys [30,31]. Thus, detailed microstructure evolutions of the alloys deformed at 440 °C and 500 °C were comparatively investigated using EBSD and TEM. It is found that the underlying mechanism of the high temperature brittleness of Mg-Gd-Y-Ag alloy was induced by segregated compounds (the Mg_3RE and Mg_2REAg phases) along the grain boundaries.

2. Materials and methods

The composition of Mg-RE alloy was Mg-10Gd-3Y-2Ag in weight percentage (wt. %). The as-cast ingot was cut into plates with dimensions of 30 mm × 20 mm × 2 mm, followed by a homogenization treatment at 500 °C for 12 h, then quenched to room temperature in silicon oil (T4 treatment). Rolling deformation was performed at 440 °C or 500 °C with a rolling speed of 20 mm/s. Before each pass, the samples were pre-heated for 30 min in a resistance furnace. The thickness reduction between each pass was ~0.1 mm.

To reveal the microstructural evolution with different rolling conditions, electron back-scattered diffraction (EBSD) characterization was performed in a scanning electron microscope (SEM, FEI Quanta 250 FEG). EBSD samples were cut from the rolling sheets. Transverse direction was set as the observation direction. The scanning step sizes are 4 μm, 0.5 μm and 0.3 μm for the sample in T4, 440 °C and 500 °C conditions. Kernel average misorientation (KAM) analysis was carried out near the cracks to reveal the nature of strain hardening [32]. Transmission electron microscopy (TEM) specimens were cut parallel to the normal plane and gently thinned to a thickness of ~25 μm. Perforation by ion milling was performed on a cold stage (~50 °C) with a low angle (<3.5°) and low energy ion beam (<3 keV). Atomic-resolution high-angle annular dark field (HAADF) observations were performed in an aberration-corrected scanning transmission electron microscope (STEM, FEI Titan G2 60-300) operated at 300 kV. Digital Micrograph plug-in was used for geometric phase analysis (GPA) to measure strain field from high-resolution TEM images. For simplicity, all the zone axes and crystal planes are hereafter referred to as those of the α-Mg matrix.

3. Results and discussions

Fig. 1a is an EBSD inverse pole figure (IPF) map of Mg-Gd-Y-Ag alloy, showing a random texture in the T4 treated sample. The grain size distribution is plotted in Fig. 1c, indicating an average grain size $\bar{d}$ of ~86 μm. The microstructure is of a typical annealed equiaxed grains with relatively clean grain interior. Fig. 1b shows the EBSD grain boundaries (GBs) map in the same observation area. Although the sample is well homogenized at 500 °C for 12 h (T4), there are still some compounds in local regions. HAADF-STEM and TEM images (Fig. 1d and e) reveal that the compounds exist mostly along grain boundaries, which are also frequently observed in other solid solute treated Mg-RE alloys with high RE contents [33,34]. X-ray diffraction (XRD) analysis indicates that the compounds are mostly the Mg_3RE and Mg_2REAg phases (Fig. 1f). These compounds are segregated at grain boundaries, but can be fragmented, refined and even dissolved during the subsequent plastic deformations [35].

Owing to their insufficient number of slip systems, Mg alloys usually show poor formability at room temperature [19,20]. We performed cold rolling on this T4 treated sample, and found that not surprisingly, cracking occurred when the thickness reduction reached 20%. To improve the formability, high temperature deformation is usually employed to activate more non-basal slip systems [30,31]. Fig. 2 shows the IPF maps of samples rolled at 440 °C with thickness reductions from 20% to 80%. During the hot deformation, defects in grain interior are significantly cleaned up through dynamic recrystallization [36,37]. Compared to the T4 sample, significant grain refinement occurred in the 20% hot rolled sample, showing an average grain size of ~33 μm (Fig. 2a). The grain size is inhomogeneous, exhibiting co-existence of coarse grains (>100 μm) and fine grains (<10 μm), which indicates that the grain refinement of 20% rolled sample is not uniform. Further deformation reduces the average grain sizes to ~25 μm, ~21 μm and ~13 μm after 40%, 60% and 80% rolling strain, as shown in Fig. 2b–d, respectively. The grain size distributions indicate that the homogeneity of grain size is improved with increasing rolling strain. Thus, Mg-Gd-Y-Ag alloys exhibit excellent formability at 440 °C, due to dynamic recrystallization. The samples are able to sustain up to 80% rolling reduction without any cracking. Similar result was also reported in the Ref. [34].

In sharp contrast, the deformation at 500 °C induced an intergranular fracture, as shown in Fig. 3a. Surprisingly, the limit of rolling reduction at 500 °C is extremely low: severe fracture occurred with only 0.5% of thickness reduction. This observation is against our general understanding that higher temperature typically improves the formability of Mg alloys. The GB map (Fig. 3b) indicates that recrystallization did not occur when the sample was deformed at 500 °C. The average grain size is ~75 μm (Fig. 3f), which is close to that of the T4 sample (~86 μm).

It is well understood that the activation of dynamic recrystallization requires two essential conditions: (1) The deformation temperature is higher than the critical recrystallization temperature; (2) The continuous straining to introduce the high density of defects. In this case, 500 °C is higher than the recrystallization temperature (440 °C). However, the defect accumulation in grain interior is very slow. Only some

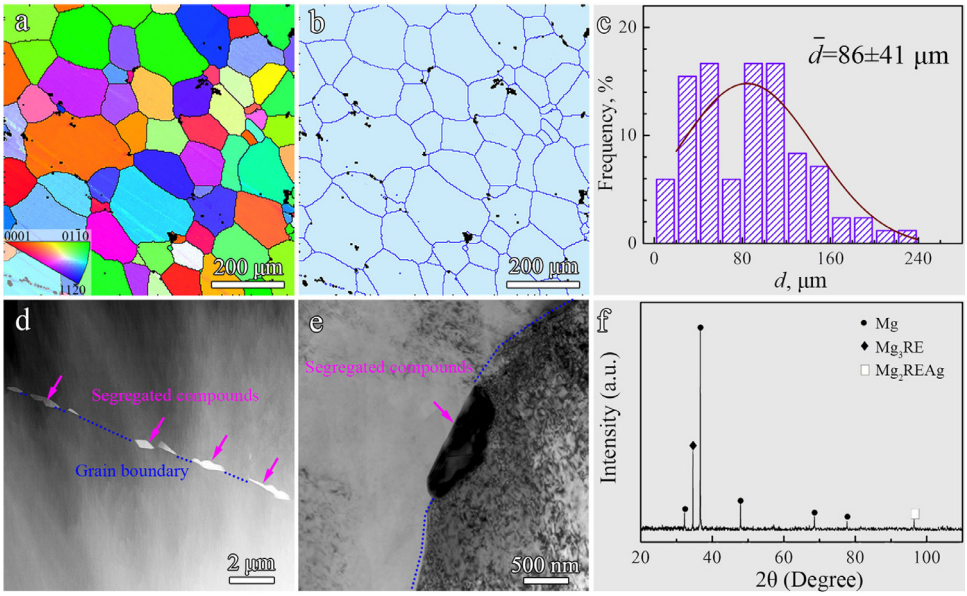

Fig. 1. Microstructure of as-received (T4 treated at 500 °C for 12 h) Mg-Gd-Y-Ag alloy: (a) IPF map, (b) GB map, (c) statistical histogram of grain size distribution, (d) HAADF-STEM image at GB, (e) bright-field TEM image at GB, (f) XRD pattern of phase constitution.

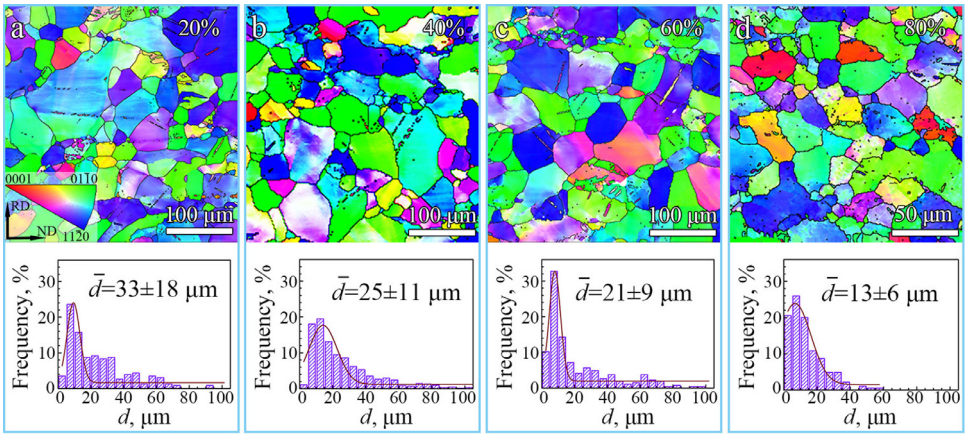

Fig. 2. EBSD IPF maps and corresponding grain size distributions of Mg-Gd-Y-Ag alloy rolled at 440 °C: (a) 20%, (b) 40%, (c) 60%, and (d) 80% of the thickness reductions.

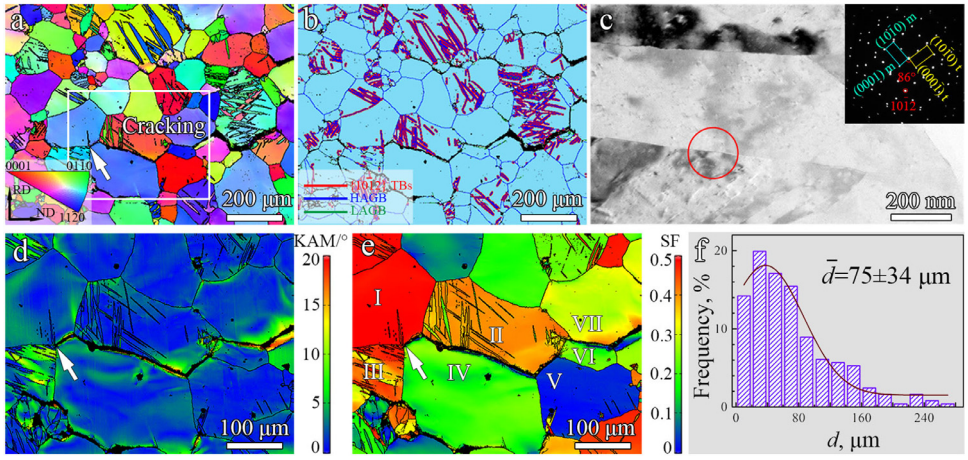

Fig. 3. Microstructure of the cracked Mg-Gd-Y-Ag alloy sample rolled at 500 °C: (a) IPF map, (b) grain boundary map, (c) TEM bright field image and corresponding diffraction pattern of twinning, (d) and (e) closed-up KAM and Schmid factor maps of the white rectangle region in (a), (f) statistical histogram of grain size distribution.

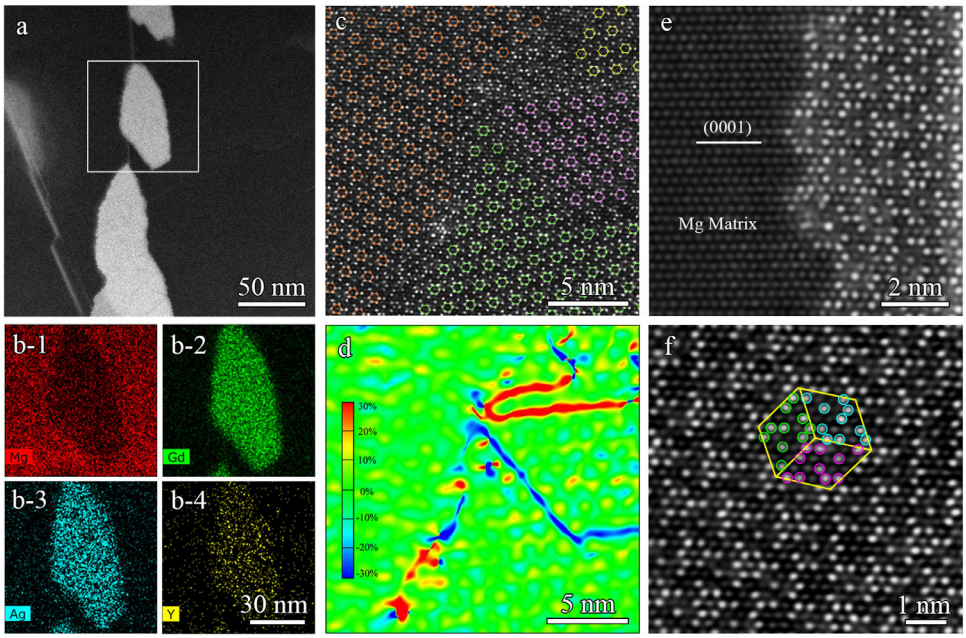

Fig. 4. Atomic-scale microstructure of the segregated compound in GB: (a) low magnification HAADF-STEM image, (b) EDS map of a specific compound, (c) high magnification HAADF-STEM image, (d) GPA analysis of lattice strain map, (e) interface between the segregated compound and matrix, (f) two-dimensional unit cell marked on a HAADF-STEM image.

deformation twins are observed in the grains along the cracks. As shown in Fig. 3c, the bright-field TEM image and corresponding SAED pattern indicate that most of them are $\{10\bar{1}2\}$ twins. Detailed analysis of deformation was carried out in the white rectangle area of Fig. 3a, using a much smaller step size of scanning. As shown in Fig. 3d, the high KAM value regions mainly distribute along the grain boundaries (7˜17°), especially along the cracks, while the KAM value in grain interior is relatively low (mostly below 2°). The Schmid factor map shows that grains (IV to VII) on both sides of the crack are below 0.3, which is unfavorable to slip activation (Fig. 3e). Fortunately, the crack growth is blocked by the grains (I to III) with higher Schmid factor (0.4˜0.5), which are easier for dislocation slip. Therefore, grain boundary sliding appear to be the main deformation mode at such a high temperature.

As mentioned above, segregated compounds exist in the T4 treated samples (Fig. 1d and e). Fig. 4a shows the HAADF-STEM image of segregated compound, which is responsible for the high temperature brittleness. The compositions of the compound have high atomic numbers, thus exhibiting a brighter contrast than that of Mg matrix [38–41]. We performed energy-dispersive X-ray spectroscopy (EDS) anaylsis, and detected all the three alloying elements in the compound(Fig. 4b). The color of the maps indicates that the concentration of Y is lower than those of Gd and Ag in the compound. Enlarged HAADF-STEM image shows that the segregated compound has a periodic structure, which has a three-fold symmetry in this zone axis (Fig. 4c). Due to the different orientations on both sides of the GB, the lattice structure of the compound is not perfect, which has lower ordering structure in some local areas. Fig. 4d is the GPA analysis of the same region, showing that the distibtion of high strain regions exist inside this compound. Owing to the high interfacial energy in disordered structure, they could be the strat area for softening at high temperature. As shown in Fig. 4e, the atomic-scale morphology of the interface between matrix and the segregated compound show a zigzag morphology, but is highly coherent in the lattice. Based on the three-fold symmetry in this zone axis, the two-dimensional unit cell of the compound is proposed as a hexagonal structure, as marked in Fig. 4f.

The segregated compounds on the grain boundary results in serious cracking, when the samples were deformed at 500 °C. Fig. 5a and b shows the segregated compounds looks like split and molten during high temperature deformation, which could be the main reason for the high temperature brittleness of the Mg-Gd-Y-Ag alloy. In general, grain boundary sliding is helpful for plastic deformation in metals, which is well studied in the researches of superplastic deformation [42–45]. However, in this specific case, the softening of the compound on the GB is equivalent to crack formation on the GB, because the molten phase can carry little stress. This statement is supported by HAADF-STEM observations that the cracking initiation occurred at the interface of segregated compounds (Fig. 5b).

Fig. 5c shows the stress-strain curves of the Mg-Gd-Y-Ag alloy compressed at 440 °C and 500 °C, respectively. The test was performed on a Gleeble-3500 thermo-mechanical simulator at a strain rate of 0.001 s^{-1}. The alloy compressed at 440 °C shows stable flow stress, which has a yield strength of ˜50 MPa. Due to the dynamic recrystallization, the flow stress shows a slight decrease after yielding, and then tends to be stable. In contrast, the stress-strain curve of the sample compressed at 500 °C shows a drastic wobble, which is

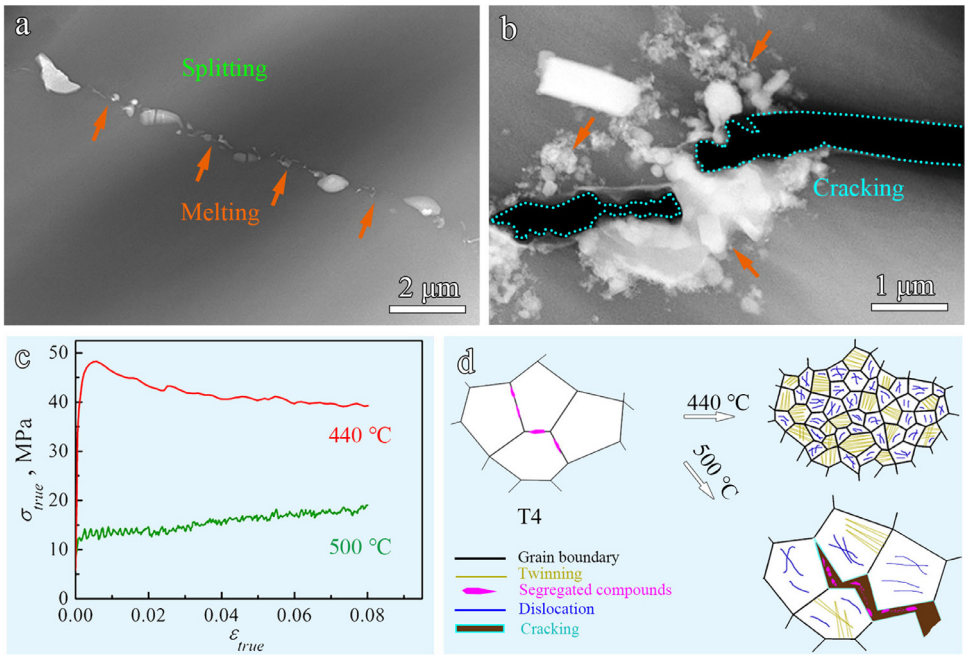

Fig. 5. Mechanism of high temperature brittleness in Mg-Gd-Y-Ag alloy: (a) HAADF-STEM of a GB, (b) growth GB cracks, (c) true stress-strain curves of hot compression at a strain rate of 0.001 s^{-1}, (d) schematic diagram of microstructure evolution deformed at 440 °C and 500 °C, respectively.

resulted from the severe cracking during the plastic deformation.

Fig. 5d illustrates the deformation mechanism of Mg-Gd-Y-Ag alloy rolled at 440 °C and 500 °C, respectively. Stable plastic deformation at 440 °C is dominated by dislocation slip and deformation twinning. Formability of the alloy is significantly improved by dynamic recrystallization, leading to grain refinement from 86 μm to 13 μm. In contrsat, at 500 °C, the softening of the compounds significnalty weakens the grain boundary, which makes it easier for the GB to slide and for the GB cracks to form, which consequently fails the sample, leading to the high temperature brittleness in the Mg-Gd-Y-Ag alloy.

To solve the high temperature brittleness, the following two methods are suggested for the processing of Mg-Gd-Y-Ag alloy. First, the content of rare earth elements in Mg-Gd-Y-Ag alloys should be reduced, which will reduce the formation of the segregated compounds along GBs. Previous work revealed that deformation of pure Mg was stable at 500 °C, even to a very high strain [46]. Second, lower the deformation temperature to avoid the softening of the compounds segregated to the GBs.

4. Conclusions

In summary, an unexpected high temperature brittleness was found in a Mg-Gd-Y-Ag alloy, which induced severe cracking under a very low deformation strain. The deformation mechanisms at different temperatures were studied. The key findings are summarized below:

(1) Segregated compound is responsible for the high temperature brittleness, which became soften during deformation at 500 °C. Cracking initiation occurs at the interface of segregated compounds. The severe cracking during deformation leads to a drastic wobble of flow stress.

(2) At 500 °C, the weakening of the grain boundaries by the softening segregated compounds led to easy grain boundary sliding. As a result, dislocation slip and accumulation in the grain interior became more difficult because the deformation was carried out largely at grain boundaries. Together with premature failure of the sample at low strain, there was not enough defects accumulated in the grain interior to initiate dynamic crystallization before sample fracture.

(3) The compositions of segregated compound have Gd, Ag and Y elements, in which the concentration of Y is lower than that of Gd and Ag. The compound has a periodic structure, which has a three-fold symmetry in the observed direction. The interface between matrix and the compound is zigzag, but is highly coherent in the lattice. The two-dimensional unit cell of the compound is proposed as have a hexagonal structure.

Acknowledgments

This work was supported by National Natural Science Foundation of China (Grant numbers 52071178, 51901103, 51931003, 51601003, 51401172), the National Key Research and Development Program of China (Grant number 2017YFA0204403), Project of Natural Science Foundation

of Heilongjiang Province (grant number LH2019E080). The authors wish to express their appreciation to the Jiangsu Key Laboratory of Advanced Micro&Nano Materials and Technology. EBSD and TEM experiments were performed at the Materials Characterization and Research Center of Nanjing University of Science and Technology.

References

[1] T.M. Pollock, Science 328 (2010) 986–987.
[2] A.A. Luo, J. Magnes. Alloy. 1 (2013) 2–22.
[3] G.S. Frankel, Nat. Mater. 14 (2015) 1189–1190.
[4] J.F. Nie, Metall. Mater. Tran. A 43 (2012) 3891–3939.
[5] J.F. Song, J. She, D.L. Chen, F.S. Pan, J. Magnes. Alloy. 8 (2020) 1–41.
[6] J.H. Zhang, S.J. Liu, R.Z. Wu, L.G. Hou, M.L. Zhang, J. Magnes. Alloy. 6 (2018) 277–291.
[7] H. Zhou, G.M. Chen, W.Z.Xu X.L.Ma, S.N. Mathaudhu, Q.D. Wang, Y.T. Zhu, Acta Mater. 95 (2015) 10–19.
[8] H. Zhou, Q.D. Wang, W. Guo, B. Ye, W.W. Jian, W.Z. Xu, X.L. Ma, J. Moering, J. Mater. Pro. Tech. 225 (2015) 310–317.
[9] K. Wei, L.R. Xiao, B. Gao, L. Li, Y. Liu, Z.G. Ding, W. Liu, H. Zhou, Y.H. Zhao, J. Magnes. Alloy. 8 (2020) 1221–1227.
[10] H Zhou, W.Z. Xu, W.W. Jian, G.M. Cheng, X.L. Ma, W. Guo, S.N. Mathaudhu, Q.D. Wang, Y.T. Zhu, in: Philos. Mag., 94, 2014, pp. 2403–2409.
[11] J.J. Bhattacharyya, F. Wang, N. Stanford, S.R. Agnew, Acta Mater. 146 (2018) 55–62.
[12] J.D. Robson, N. Stanford, M.R. Barnett, Acta Mater. 59 (2011) 1945–1956.
[13] B.Y. Liu, N. Yang, J. Wang, M. Barnett, Y.C. Xin, D. Wu, R.L. Xin, Bin. Li, R.L. Narayan, J.F. Nie, J. Li, E. Ma, Z.W. Shan, J. Mater. Sci. Tech. 34 (2018) 1061–1066.
[14] X.C. Sha, L.R. Xiao, X.F. Chen, G.M. Chen, Y.D. Yu, D.D. Yin, H. Zhou, Philos. Mag. 99 (2019) 1957–1969.
[15] Z.L. Ning, J.Y. Yi, M. Qian, H.C. Sun, F.Y. Cao, H.H. Liu, J.F. Sun, Mater. Des. 60 (2014) 218–225.
[16] J.M. Jiang, S. Ni, H.G. Yan, N. Yan, M. Song, Scripta Mater 170 (2019) 24–28.
[17] S.Q. Zhu, S.P. Ringer, Acta Mater. 144 (2018) 365–375.
[18] N. Stanford, M.R. Barnett, Int. J. Plast. 47 (2013) 165–181.
[19] Z. Wu, W.A. Curtin, Acta Mater. 88 (2015) 1–12.
[20] Z. Wu, W.A. Curtin, Nature 526 (2015) 62–67.
[21] L. Gao, R.S. Chen, E.H. Han, J. Alloy. Compds. 472 (2009) 234–240.
[22] Y.J. Cui, Y.P. Li, Z.C. Wang, X. Ding, Y. Koizumi, H.K. Bian, L.Y. Lin, A. Chiba, Int. J. Plast. 91 (2017) 134–159.
[23] H. Zhou, Q.D. Wang, B. Ye, W. Guo, Mater. Sci. Eng. A 576 (2013) 101–107.
[24] R. Alizadeh, R. Mahmudi, P.H.R. Pereira, Y. Huang, T.G. Langdon, Mater. Sci. Eng. A 682 (2017) 577–585.
[25] H. Zhou, H.Y. Ning, X.L. Ma, D.D. Yin, L.R. Xiao, X.C. Sha, Y.D. Yu, Q.D. Wang, Y.S. Li, J. Mater. Sci. Tech. 34 (2018) 1067–1075.
[26] X.X. Dong, L.Y. Feng, S.H. Wang, E.A. Nyberg, S.X. Ji, J. Magnes. Alloy. 9 (2021) 90–101.
[27] L.R. Xiao, Y. Cao, S. Li, H. Zhou, X.L. Ma, L. Mao, X.C. Sha, Q.D. Wang, Y.T. Zhu, X.D. Han, Acta Mater 162 (2019) 214–225.
[28] H. Sun, Z.G. Ding, D.L. Zhang, H. Zhou, S. Li, E.J. Lavernia, Y.T. Zhu, W. Liu, Materialia 7 (2019) 100352.
[29] K. Wei, R. Hu, D.D. Yin, L.R. Xiao, S. Pang, Y. Cao, H. Zhou, Y.H. Zhao, Y.T. Zhu, Acta Mater. 206 (2021) 116604.
[30] A. Chapuis, J.H. Driver, Acta Mater. 59 (2011) 1986–1994.
[31] W.B. Hutchinson, M.R. Barnett, Scripta Materialia 63 (2010) 737–740.
[32] X.L. Liu, Q.Q. Xue, W. Wang, L.L. Zhou, P. Jiang, H.S. Ma, F.P. Yuan, Y.G. Wei, X.L. Wu, Materialia 7 (2019) 100376.
[33] F. Khan MD, S.K. Panigrahi, J. Magnes. Alloy. 3 (2015) 210–217.
[34] H.Y. Ning, Y.D. Yu, B. Gao, L.R. Xiao, L.H. Wen, Z.H. Yan, L. Li, X.F. Chen, Materials 11 (2018) 757.
[35] W. Fu, R.H. Wang, H. Xue, J. Kuang, J.Y. Zhang, G. Liu, J. Sun, J. Alloy. Compds. 747 (2018) 197–210.
[36] Y.T. Zhu, X.L. Wu, App. Phy. Lett. 89 (2006) 031922.
[37] L.R. Xiao, X.F. Chen, Y. Cao, H. Zhou, X.L. Ma, D.D. Yin, B. Ye, X.D. Han, Y.T. Zhu, Scripta Mater. 177 (2020) 69–73.
[38] J.F. Nie, Y.M. Zhu, J.Z. Liu, X.Y. Fang, Science 340 (2013) 957–960.
[39] X.J. Zhao, H.W. Chen, N. Wilson, Q. Liu, J.F. Nie, Nat. Commun. 10 (2019) 3243.
[40] X.F. Chen, L.R. Xiao, D.G. Ding, W. Liu, Y.T. Zhu, X.L. Wu, Scripta Mater. 178 (2020) 193–197.
[41] L.R. Xiao, X.F. Chen, K. Wei, Y. Liu, D.D. Yin, Z.H. Hu, H. Zhou, Y.T. Zhu, Scripta Mater. 191 (2021) 219–224.
[42] K.D. Molodov, D.A. Molodov, Acta Mater. 153 (2018) 336–353.
[43] S.S. Jiang, Y. Jia, X.J. Wang, J. Magnes. Alloy. 8 (2020) 1186–1197.
[44] A.D. Sheikh-Ali, Acta Mater. 58 (2010) 6249–6255.
[45] H. Yoshida, K. Yokoyama, N. Shibata, Y. Ikuhara, T. Sakuma, Acta Mater. 52 (2004) 2349–2357.
[46] Y. Chino, M. Kado, M. Mabuchi, Acta Mater. 56 (2008) 387–394.